Defining the genes required for survival of *Mycobacterium bovis* in the bovine host offers novel insights into the genetic basis of survival of pathogenic mycobacteria

Amanda J Gibson[1,5&*], Jennifer Stiens[2*], Ian J Passmore[3], Valwynne Faulkner[1,6&], Josephous Miculob[1], Sam Willcocks[3], Michael Coad[4], Stefan Berg[4], Dirk Werling[1], Brendan W Wren[3], Irene Nobeli[2], Bernardo Villarreal-Ramos[4,5&], Sharon L Kendall[1**]

[1]Centre for Emerging, Endemic and Exotic Diseases, Pathobiology and Population Sciences, Royal Veterinary College, Hawkshead Lane, North Mymms, Hatfield, AL9 7TA, United Kingdom.

[2]Institute of Structural and Molecular Biology, Biological Sciences, Birkbeck, University of London, Malet Street, London, WC1E 7HX, United Kingdom.

[3]London School of Hygiene and Tropical Medicine, Keppel Street, London, WC1E 7HT, United Kingdom.

[4]Animal and Plant Health Agency, Woodham Ln, Addlestone, Surrey, KT15 3NB, United Kingdom.

[5]Centre of Excellence for Bovine Tuberculosis, IBERS, Aberystwyth University, Penglais, Aberystwyth, Ceredigion, SY23 3EE, United Kingdom.

[6]Systems Chemical Biology of Infection and Resistance Laboratory, The Francis Crick Institute, 1 Midland Road, London 15 NW1 1AT, United Kingdom.

[&] current address

*the authors contributed equally to the work

**corresponding author

Abstract

Tuberculosis has severe impacts in both humans and animals. Understanding the genetic basis of survival of both *Mycobacterium tuberculosis*, the human adapted species, and *Mycobacterium bovis*, the animal adapted species is crucial to deciphering the biology of both pathogens. There are several studies that identify the genes required for survival of *M. tuberculosis in vivo* using mouse models, however, there are currently no studies probing the genetic basis of survival of *M. bovis in vivo.* In this study we utilise transposon insertion sequencing in *M. bovis* to determine the genes required for survival in cattle. We identify genes encoding established mycobacterial virulence functions such as the ESX-1 secretion system, PDIM synthesis, mycobactin synthesis and cholesterol catabolism that are required *in vivo*. We show that, as in *M. tuberculosis, phoPR* is required by *M. bovis in vivo* despite the known defect in signalling through this system. Comparison to studies performed in glycerol adapted species such as *M. bovis* BCG and *M. tuberculosis* suggests that there are differences in the requirement genes involved in cholesterol import (*mce4* operon), oxidation (*hsd*) and detoxification (*cyp125*). We report good correlation with existing mycobacterial virulence functions, but also find several novel virulence factors, including genes involved in protein mannosylation, aspartate metabolism and glycerol-phosphate metabolism. These findings further extend our knowledge of the genetic basis of survival *in vivo* in bacteria that cause tuberculosis and provide insight for the development of novel diagnostics and therapeutics.

45 **Importance**

46 This is the first report of the genetic requirements of an animal adapted member of
47 the MTBC in a natural host. *M. bovis* has devastating impacts in cattle and bovine
48 tuberculosis is a considerable economic, animal welfare and public health concern. The data
49 highlight the importance of mycobacterial cholesterol catabolism and identifies several new
50 virulence factors. Additionally, the work informs the development of novel differential
51 diagnostics and therapeutics for TB in both human and animal populations.

52

53 **Introduction**

54 Bacteria belonging to the *Mycobacterium tuberculosis* complex (MTBC) have
55 devastating impacts in both animal and human populations. *Mycobacterium bovis,* an
56 animal adapted member of the MTBC and one of the main causative agents of bovine
57 tuberculosis (bTB), remains endemic in some high-income settings despite the
58 implementation of a test and slaughter policy. In low- and middle-income settings, the
59 presence of bTB in livestock combined with the absence of rigorous control measures
60 contributes to the risk of zoonotic transmission (1, 2). Control measures based on cattle
61 vaccination utilise the live attenuated vaccine *M. bovis* BCG but the efficacy of this vaccine
62 still remains low in field situations (3, 4). In addition to vaccines, the development of
63 diagnostic tools for the identification of infected individuals is crucial for the management of
64 transmission. Currently, vaccination with *M. bovis* BCG sensitises animals to the diagnostic
65 tuberculin skin test, therefore, sensitive and specific differentiating diagnostic strategies are
66 a current imperative (5, 6).

67 The increased accessibility of whole genome fitness screens has allowed the
68 assessment of the impacts of the loss of gene function on bacterial survival (7). Such screens
69 have been invaluable in identifying novel drug targets or candidates for the generation of
70 new live attenuated vaccines in a number of bacterial pathogens, including *Mycobacterium*
71 *tuberculosis* (8–13). Studies utilising whole genome transposon mutagenesis screens to
72 examine gene fitness *in vivo* in *M. tuberculosis* have been limited to mouse models (8, 9,
73 13). These models do not faithfully replicate the granulomatous pathology associated with
74 TB, nor do mice contain the same repertoire of CD1 molecules expressed by bovine T cells
75 required to present mycobacterial lipid antigens (14). Whole genome transposon
76 mutagenesis screens utilising non-human primates are limited because screening is
77 restricted to smaller mutant pools (15). To date, Tn-seq based studies in the context of bTB
78 in cattle have only been performed using *M. bovis* BCG strains (16, 17).

79 In this study we use transposon insertion sequencing (Tn-seq) to determine the
80 genes required for survival of *M. bovis* directly in cattle. We show that genes involved in the
81 biosynthesis of phthiocerol dimycocerosates (PDIMs), the ESX-1 secretion system,
82 cholesterol catabolism, and mycobactin biosynthesis are essential for survival *in vivo* in
83 cattle, corroborating current knowledge of gene essentiality in members of the MTBC (8, 9,
84 13, 16, 17). We identify differences in the requirement for genes involved in cholesterol
85 transport and oxidation in the fully virulent *M. bovis* strain. We also identify several novel
86 genes required for survival *in vivo* that have not been previously described in members of
87 the MTBC.

88

89 **Results and Discussion**

90 **Generation and sequencing of the input library.**

91 We generated a transposon library in *M. bovis* AF2122/97 using the MycomarT7 phagemid
92 system as previously described (18, 19). Sequencing of the input library showed that
93 transposon insertions were evenly distributed around the genome and 27,751 of the
94 possible 73,536 thymine–adenine dinucleotide (TA) sites contained an insertion
95 representing a saturation density of ~38% (Supplementary Figure S1 and Supplementary
96 Table S1 -input library). The *M. bovis* AF2122/97 genome has 3,989 coding sequences and
97 insertions were obtained in 3,319 of these, therefore the input library contained insertions
98 in 83% of the total coding sequences.

99

100 ***Mycobacterium bovis* specific immune responses were observed in cattle**

101 Twenty-four clinically healthy calves of approximately 6 months of age were inoculated with
102 the library through the endobronchial route. Infection was monitored by IFN-γ release assay
103 (IGRA) at the time of inoculation and 2 weeks post infection. *M. bovis* specific immune
104 responses were observed for all study animals at 2 weeks post infection (Figure 1A and B).
105 Each animal presented very low background of circulating IFN-γ together with a statistically
106 significant increase in IFN-γ release in response to PPD-B compared to PPD-A antigens
107 (Figure 1C; *** $p \leq 0.001$). This indicates that infection with the library was successfully
108 established in the cattle.

109

110 **Pathology associated with infection was greater in the lung and thoracic lymph nodes**

111 Animals were culled at 6 weeks post infection. Lung sections and upper (head and neck) and
112 lower (thoracic) respiratory tract associated lymph nodes were examined for gross lesions.
113 Lesions typical of *M. bovis* infection were observed in the tissues examined. Pathology
114 scores are shown in Figure 2A. Greater pathology was observed in lung and thoracic lymph
115 nodes compared to the head and neck lymph nodes.

116

117 **Higher bacterial loads were associated with the lung and thoracic lymph nodes**

118 Bacterial counts were highest in lesions derived from the lung compared to those from the
119 thoracic lymph nodes and head and neck lymph nodes (Figure 2B). The lowest bacterial
120 counts were observed within the head and neck lymph nodes. However, this was not
121 significant when compared to thoracic lymph nodes. The volume of each macerate varied
122 depending on lesion size. Considering macerate volume, average bacterial loads of 10^7, 10^6
123 and 10^5 were recovered from lesions from samples of the lungs, thoracic lymph nodes and
124 head and neck lymph nodes, respectively.

125

126 **Recovery and sequencing of *in vivo* selected transposon libraries**

127 In order to recover the Tn library from harvested tissue ~ 10^5 -10^6 CFU from lungs and
128 thoracic lymph nodes were plated onto several 140 mm modified 7H11 plates containing
129 kanamycin to minimize competition between mutants. Samples from 4 cattle were lost due
130 to fungal contamination, therefore the samples processed represent samples from 20 cattle.
131 Lung samples were plated from all 20 animals and thoracic lymph nodes samples were
132 plated from 6 cattle. Bacteria were grown for 4-6 weeks before harvesting for genomic DNA

133 extraction and subsequent sequencing (see Supplementary Table S1 for assignation of
134 sequencing files to samples). The diversities of the output libraries were compared to the
135 input library for each sample (Supplementary Figure S2 and Table S1). On average, libraries
136 recovered from lung lesions from 20 different cattle contained 14,456 unique mutants and
137 those recovered from the thoracic lymph nodes contained an average of 16,210 unique
138 mutants. Given that the input library contained 27,751 unique mutants this represented a
139 loss of diversity of ~ 40-50%. Good coverage of coding sequences (CDSs) was maintained as
140 the output libraries still contained insertions in (on average) 68-70% of the open reading
141 frames.

142 Comparison of the read counts between the input and output libraries allowed a
143 measurement of the impact of the insertion on the survival of mutants in cattle. The results
144 are represented as a mean $\log_2$ fold-change in the output compared with the input for each
145 gene. The entire dataset is shown in supplementary Table S4 and a volcano plot from the
146 lungs and thoracic lymph node of two representative animals is shown in Supplementary
147 Figure S3. Comparison of the mean $\log_2$ fold-change between lung and lymph node samples
148 showed good correlation (Spearman's rho = 0.88, p-value <2.2e-16) (Supplementary Figure
149 S4). TRANSIT resampling was performed to compare the composition of the mutant
150 population in the lungs and thoracic lymph nodes of paired cattle, it was also applied to
151 compare all the thoracic lymph nodes with the lungs of all cattle samples. No statistically
152 significant differences were observed indicating that there were no differences in mutant
153 composition between the tissue sites.

154 No insertion mutants were significantly over-represented in the output library in any
155 of the animals. Although interestingly, insertions in *MB0025,* a gene that is unique to *M.*

156 *bovis* appeared to improve growth in cattle as mean $\log_2$ fold-changes of +3.9 (lungs) and
157 +4.2 (lymph nodes) were observed; however, significance criteria were not met in any of the
158 animals.

159 In order to define a list of attenuating mutations, we used a similar approach to that
160 used in a previous study with an *M. bovis* BCG library in cattle (16). Insertions in genes were
161 defined as attenuating if they had $\log_2$ fold-change of -1.5 or below and an adjusted p-value
162 of <0.05 in at least half of the animals (Table S4, significant in 50% of cattle tab). When using
163 these criteria, there were 141 genes where insertions caused significant attenuation in the
164 lungs or the thoracic lymph nodes, 20 genes that reached significance only in the lungs
165 (shown in red) and 16 genes that reached significance only in the thoracic lymph nodes
166 (shown in green). Of the 141 genes, 109 had been previously described as being required *in*
167 *vivo* in *M. tuberculosis* H37Rv in mouse models through the use of whole genome Tn
168 screens representing ~77% overlap with the previous literature (8, 9, 13).

169

170 **Comparison with mutations known to cause attenuation in the MTBC**

171 Insertions in the RD1 encoded ESX-1 type VII secretion system secreting virulence
172 factors and immunodominant antigens EsxA (CFP-10) and EsxB (ESAT-6) are expected to
173 cause attenuation (20). The impacts of insertions in this region are summarised in Figure 3
174 but are also available in Supplementary Table S4 (RD regions tab) and Supplementary Figure
175 S5. Insertions in genes encoding the structural components of the apparatus (*eccB1, eccCa1,*
176 *eccCb1, eccD1*) were severely attenuating ($\log_2$ fold-change -6 to -9). Insertions in *eccA1,*
177 which also codes for a structural component of the apparatus, were less impactful ($\log_2$ fold-
178 changes of -2 to -3) despite good insertion saturation in this gene. This is supported by the

179 work of others who have shown that deletion of *eccA1* in *Mycobacterium marinum* leads to
180 only a partial secretion defect (21). There were no impacts seen due to insertions in
181 accessory genes *espJ, espK* and *espH.* The lack of attenuation seen in *espK* mutants is
182 supported by other studies showing that this gene is dispensable for secretion through the
183 apparatus and is not required for virulence of *M. bovis* in guinea pigs (22, 23). Insertions in
184 *esxA* and *esxB* resulted in severe attenuation ($\log_2$ fold-change of -6) but this did not reach
185 significance cut-offs (adj. p=<0.05) in any of the cattle. This is likely to be due to the small
186 number of TAs in these genes which makes it challenging to measure mutant frequency.

187 The highest levels of attenuation seen were in genes involved in the synthesis of the
188 cell wall virulence lipids PDIMs (*ppsABCDE* and *mas* with $\log_2$ fold-changes of ~-10
189 commonly seen). PDIM synthesis is well known to be required for the survival of *M.*
190 *tuberculosis* and *M. bovis* in mice and guinea pigs (24, 25). Insertions in genes involved in
191 the synthesis of PDIMs were the most under-represented ($\log_2$ fold-changes of -8 to -10) in
192 the output library (Figure 4, Supplementary Table S4, mycolipids tab). MmpL7 is involved in
193 PDIM transport and there is evidence that it is phosphorylated by the serine-threonine
194 kinase PknD (26). PknD-MmpL7 interactions are thought to be perturbed in *M. bovis* as *pknD*
195 is split into two coding sequences in the bovine pathogen by a frameshift mutation (27). The
196 data presented here suggest that MmpL7 still functions despite the frameshift mutation.

197 Iron restriction is thought to be a mechanism by which the host responds to
198 mycobacterial infection, although different cellular compartments may be more restrictive
199 than others (28). Insertion in many of the genes involved in mycobactin synthesis *(Mb2406-*
200 *Mb2398, mbtJ-mbtH)* were attenuating in cattle (Figure 4, Supplementary Table S4,
201 mycobactin synthesis tab). As mycobactin is required for the acquisition of iron, this

202 confirms that, like other members of the MTBC, needs to scavenge iron from the host for
203 survival (13, 16).

204 The role of the cholesterol catabolism in *M. tuberculosis* is well documented and it is
205 required for both energy generation and manipulation of the immune response (29–31).
206 Cholesterol uptake is mediated by the Mce4 transporter coded by the *mce4* operon
207 *Rv3492c-Rv3501c* (*Mb3522c-MB3531c*) (32, 33). It has been suggested that an alternative
208 cholesterol acquisition pathway operates in *M. bovis* BCG Danish as, unlike insertions in
209 genes in the down-stream catabolic pathway, insertions in the *mce4* operon do not result in
210 attenuation in this strain (16). In contrast, our study shows that cholesterol transport via the
211 Mce4 transporter is required in *M. bovis* (Figure 4, Supplementary Table S4 -cholesterol
212 catabolism tab, Figure 5). This corroborates work performed in *M. tuberculosis*, where Mce4
213 has been shown to be required for growth in chronically infected mice (9, 32). Propionyl-coA
214 generated from the catabolism of cholesterol is toxic and detoxification mechanisms include
215 incorporation into PDIMs (34, 35). The observation that BCG Danish contains a lower
216 amount of PDIMs compared to BCG Pasteur (16) suggests a correlation between Mce4
217 mediated cholesterol transport and PDIM synthesis and previous studies have
218 demonstrated an increase in PDIM biosynthesis as a result of *mce4* over-expression (36).
219 PDIMs biosynthesis genes are over-expressed in *M. bovis* compared to *M. tuberculosis* (27)
220 and comparison of our dataset with Tn-seq studies performed in *M. tuberculosis* (9)
221 indicates an over-reliance of *M. bovis* on cholesterol transport through the Mce4
222 transporter (Figure 5).

223 Early stages of cholesterol catabolism involve the oxidation of cholesterol to
224 cholestenone, a reaction catalysed by the 3β-hydroxysteroid dehydrogenase (*hsd*) encoded

225 by *Rv1106c/Mb1136c* (37). The cytochrome P450 Cyp125 (*Mb3575c/Rv3545c*) is required
226 for the subsequent detoxification of cholestenone (38). Insertions in both *hsd* and *cyp125* in
227 *M. bovis* were severely attenuating with $\log_2$ fold-changes of ~-5 to -7 (Supplementary Table
228 S4 - cholesterol catabolism tab, Figure 5). Previous studies have shown that these genes are
229 not required for the survival of *M. tuberculosis* in macrophages or in guinea pigs and this is
230 thought to be due to the availability of other carbon sources, including glycolytic substrates,
231 *in vivo* (37, 39–43). *M. bovis* is more restricted in metabolic capabilities and is unable to
232 generate energy from glycolytic intermediates, largely due to a disrupted pyruvate kinase
233 encoded by *pykA* (44, 45). The essentiality of *hsd* and *cyp125* during infection for *M. bovis*
234 but not *M. tuberculosis* supports the hypothesis of an over-reliance of *M. bovis* on
235 cholesterol. Given the potential for the use of host cholesterol metabolites as diagnostic
236 biomarkers, this observation might have applications in the development of differential
237 diagnostics (46).

238

239 **Genes that are differentially expressed between *Mycobacterium bovis* and**
240 ***Mycobacterium tuberculosis*.**

241 Several studies have identified key expression differences between *M. bovis* and *M.*
242 *tuberculosis* (27, 47, 48). We examined the dataset for insights on the role of differentially
243 expressed genes and transcriptional regulators during infection. One important regulatory
244 system in *M. tuberculosis* is the two-component regulatory system PhoPR and deletions in
245 the *phoPR* genes alongside *fadD26* are attenuating mutations in the live vaccine MTBVAC
246 (49–51). Our data show that insertions in both *phoPR* and *fadD26* were severely attenuating
247 with $\log_2$ fold-changes of -6 to -9 (Figure 6, Supplementary Table S4, *phoPR* regulon tab and
248 mycolipids tab). This reinforces the role of this system in virulence, despite the presence of a

249 single nucleotide polymorphism (SNP) in the sensor kinase *phoR* that impacts signalling
250 through the system in *M. bovis* (52). Signal potentiation via *phoR* is required for secretion of
251 ESAT-6 through the ESX-1 secretory system and *M. bovis* is known to have compensatory
252 mutations elsewhere in the genome, e.g. in the *espACD* operon, that restores ESAT-6
253 secretion in the face of a deficient signalling system (49, 52, 53). Our data also show that Tn
254 insertions in *espA* of the *espACD* operon (required for ESAT-6 secretion) and in *mprA*, a
255 transcriptional regulator of that operon (54) were severely attenuating (log2 fold-changes -7
256 to -9), emphasising the relevance of ESAT-6 as a virulence factor.

257 Studies comparing differences in expression during *in vitro* growth between *M. bovis*
258 and *M. tuberculosis* show that genes involved in sulfolipid (SL-1) biosynthesis are expressed
259 at lower levels in *M. bovis* compared to *M. tuberculosis* (27, 47). Interestingly, insertions in
260 genes involved in SL-1 biosynthesis (*Mb3850-Mb3856*) are not attenuating *in vivo*
261 (Supplementary File S4, mycolipids tab), reinforcing the lack of importance of SL-1 for *M.*
262 *bovis in vivo,* at least at the stages of infection studied here.

263 One of the most highly attenuating insertions occurred in *Mb0222/Rv0216* ($\log_2$ fold
264 change –8 to -9). This gene has been shown to be highly (> 10-fold) over-expressed in *M.*
265 *bovis* compared with *M. tuberculosis* but the physiological function of this gene is not
266 currently known. The secreted antigens MPB70 and MPB83, encoded by *Mb2900* and
267 *Mb2898* are also over-expressed in *M. bovis* and play a role in host-specific immune
268 responses, however, insertions in these genes did not cause attenuation *in vivo* in our
269 dataset (55).

270

271 **Novel attenuating mutations**

272 We identified 32 genes that were required for survival of *M. bovis* in cattle that had not
273 been previously described as being essential *in vivo* through transposon mutagenesis
274 screens of *M. tuberculosis* in mouse models (8, 9, 13) (see Supplementary Table 4,
275 Significant in 50% of cattle tab). While writing this publication, a large scale Tn-seq study
276 that utilised over 120 *M. tuberculosis* libraries and several diverse mouse genotypes (the
277 collaborative cross mouse panel (56)) showed that the panel of genes required for the
278 survival of *M. tuberculosis in vivo* is much larger than previously reported (57). A direct
279 comparison of our dataset with the study by Smith et al., revealed that a further 13 genes
280 were shown to be required in at least one mouse strain in that study. A summary set of the
281 remaining 19 genes is given in Supplementary Table 4, Not in Mtb Tn-seqs tab. Some of
282 these genes have been shown to be attenuated in the mouse model in *M. tuberculosis*
283 through the use of single mutants (58–61).

284 Included in this list are genes required for phenolic glycolipid synthesis. Insertions in
285 *Mb2971c/Rv2947c* (*pks15/1*) and in *Mb2972c/Rv2948c* (*fadD22*) were attenuating in *M.*
286 *bovis* but these genes are not required *in vivo* in *M. tuberculosis,* including in the extended
287 panel of mouse genotypes (8, 9, 13, 57). Both *pks15/1* and *fadD22* are involved in the early
288 stages of synthesis of phenolic glycolipids (PGLs) and are involved in virulence (62). The
289 requirement for these genes in *M. bovis* but not in *M. tuberculosis* is consistent with the
290 observation that the Tn-seq studies in *M. tuberculosis* are often carried out using lineage 4
291 strains (H37Rv and CDC1551) that harbour a frameshift mutation in the *pks15/1* gene, which
292 renders them unable to synthesise PGLs. This removes the requirement for these genes *in*
293 *vivo* in lineage 4 strains of *M. tuberculosis. pks15/1* has been previously reported to be
294 required for survival of *M. bovis* in a guinea pig model of infection (63).

295 The list also includes genes that are involved in post-translational modifications such
296 as glycosylation. *Rv1002c* is thought to add mannose groups to secreted proteins and over-
297 expression of this protein in *M. smegmatis* was recently shown to enhance survival *in vivo*
298 and inhibit pro-inflammatory cytokine production (64). The substrates of this protein
299 mannosyltransferase are thought to be several secreted lipoproteins, including LpqW which
300 is involved in the insertion of the virulence lipid LAM at the mycobacterial cell surface (64,
301 65).

302 Finally, this list includes two genes (*aspC* and *glpD2*) that are essential *in vitro* in *M.*
303 *tuberculosis* but not in *M. bovis* (10, 11, 18, 66). Information regarding *aspC* and *glpD2* from
304 Tn-seq approaches is likely to be lacking in *M. tuberculosis* because Tn mutants will not be
305 represented in the input pool. The absence of insertion mutants in these genes in the most
306 recent large-scale *M. tuberculosis* Tn-seq study supports this (57). One of these genes
307 *MB0344c/Rv0337c* (*aspC*) is an aspartate aminotransferase involved in the utilisation of
308 amino acids (aspartate) as a nitrogen source (67). The other gene *Mb3303c/Rv3302c* (*glpD2*)
309 is a membrane bound glycerol-phosphate dehydrogenase. In *Escherichia coli*, *glpD2* is an
310 essential enzyme, functioning at the central junction of respiration, glycolysis, and
311 phospholipid biosynthesis and catalyses the oxidation of dihydroxyacetone phosphate
312 (DHAP) from glycerol-3-phosphate resulting in the donation of electrons to the electron
313 transport chain (68). Its essentiality *in vitro* in *M. tuberculosis* might be explained by the
314 usage of glycerol during *in vitro* growth in this species. The contribution of the membrane
315 bound *glpD2* in donation of electrons to the electron transport chain, has been suggested
316 but not yet explored in the MTBC (69). Given the interest in the electron transport chain as a
317 chemotherapeutic target in *M. tuberculosis*, the data presented here suggests that
318 inhibition of *glpD2* might be a fruitful approach in the development of new drugs for the

319 treatment of TB in humans (70). The role of this gene in *M. bovis in vivo* is perhaps
320 surprising, given the disruptions in glycerol phosphate uptake and pathways that
321 phosphorylate glycerol in *M. bovis* AF2122/97 (71). However, *M. tuberculosis* is thought to
322 engage in catabolism of membrane derived glycerophospholipids which may be a potential
323 source of glycerol-3-phosphate in members of the complex (72).

324

325 **Materials and Methods**

326 **Bacterial strains and culture methods**

327 *M. bovis* strain AF2122/97 was maintained on modified Middlebrook 7H11 (BD Difco™)
328 medium (73). Liquid cultures of *M. bovis* were grown in Middlebrook 7H9 media (BD
329 Difco™) containing 75 mM sodium pyruvate, 0.05% v/v Tween®80 and 10% Middlebrook
330 albumin-dextrose-catalase (ADC) (BBL BD Biosciences). Kanamycin at 25 µg/ml was used for
331 selection where appropriate.

332

333 **Generation of input transposon mutant library and preparation of the inoculum**

334 Transposon libraries in *M. bovis* were generated as previously described using the
335 MycomarT7 phagemid system as per Majumdar et al with modifications (19). Approximately
336 66,000 kanamycin resistant transductants were scraped and homogenised in 7H9 medium
337 and stored frozen at -80°C in 1 ml aliquots. CFU counting was performed on the
338 homogenised culture to inform inoculum dosage.

339

340 **Cattle Infection**

341 Experiments were carried out according to the UK Animal (Scientific Procedures) Act 1986
342 under project license PPL70/7737. Ethical permission was obtained from the APHA Animal
343 Welfare Ethical Review Body (AWERB) (UK Home Office PCD number 70/6905). All animal
344 infections were carried out within the APHA large animal biocontainment level 3 facility.
345 Twenty-four Holstein-Friesian crosses of 6 months of age were sourced from an officially TB-
346 free herd. An infectious dose of 7 x 10^4 CFU was targeted for the "input" library, allowing
347 each mutant to be represented in the library ~ 2.5-fold. Retrospective counting of the
348 inoculum revealed the actual inoculum for infection contained 4 x 10^4 CFU. The inoculum
349 was delivered endobronchially in 2 ml of 7H9 medium. In brief, animals were sedated with
350 xylazine (Rompun® 2%, Bayer, France) according to the manufacturer's instructions (0.2
351 mL/100 kg, IV route) prior to the insertion of an endoscope through the nasal cavity into the
352 trachea for delivery of the inoculum through a 1.8 mm internal diameter cannula
353 (Veterinary Endoscopy Services, U.K.) above the bronchial opening to the cardiac lobe and
354 the main bifurcation between left and right lobes.

355

356 **Infection Monitoring with the IFN-γ release Assay (IGRA)**

357 Blood was collected by jugular venepuncture from animals on the day of the infectious
358 challenge and two weeks after infection. Heparinized whole blood (250 µl) was incubated
359 with purified protein derivative (PPD) from *M. avium* (PPD-A) or PPD from *M. bovis* (PPD-B)
360 (Prionics™) respectively at 25 IU and 30 IU final. Pokeweed mitogen was used as the positive
361 control at 10 µg/mL and a medium-only negative control. After 24 h incubation in 5% (v/v)
362 CO_2, 95% humidity, 37 °C atmosphere bloods were centrifuged (400 × *g* for 5 min); 120 µl

363 of supernatant was removed and stored at −80°C for subsequent IFN-γ quantification using
364 the BOVIGAM® kit (Prionics™) in accordance with the manufacturer's instructions.

365

366 **Collection of tissues and gross pathology scores**

367 Six weeks after the initial infection animals were subjected to post-mortem examination.
368 Initially the experiment was designed with two time points; an early time point (6 weeks)
369 and a later time point of 8 weeks. However, due to the unexpected high-levels of pathology
370 seen at the earlier time-points all animals were culled at 6 weeks. Gross pathology and
371 evidence of TB-like granulomas lesions was scored using a modified methodology to that
372 previously described in (74). Tissue from head and neck lymph nodes (from the right and left
373 sub-mandibular lymph nodes, the right and left medial retropharyngeal lymph nodes),
374 thoracic lymph nodes (the right and left bronchial lymph nodes, the cranial tracheobronchial
375 lymph nodes, the cranial and caudal mediastinal lymph nodes) and from lung lesions, was
376 collected into sterile containers and frozen at −80°C until further processing. Frozen tissues
377 were thawed and homogenised in PBS using a Seward Stomacher Paddle Blender.

378

379 **Recovery of the output transposon mutant library from tissues**

380 Tissue macerates collected from study animals were thawed at room temperature, diluted
381 in PBS and plated on modified 7H11 agar to determine bacterial loads. Colony counts were
382 performed after 3-4 weeks growth. For recovery of the library from tissue macerates ~10^5-
383 10^6 CFU were plated from lung lesions and thoracic lymph node lesions onto modified 7H11
384 media containing 25 µg/ml kanamycin. The colonies were plated over several 140 mm petri

385 dishes to minimise competition between mutants. The colonies were harvested after 4-6
386 weeks growth and genomic DNA extracted.

387

388 **Genomic DNA extraction**

389 Genomic DNA from the input and recovered libraries was isolated by an extended bead
390 beating procedure with detergent-based lysis, phenol-chloroform DNA extraction and
391 precipitation as previously described (18). DNA quality was assessed by nano-spectrometry
392 (DeNovix) and gel electrophoresis and quantified by Qubit analysis using the Broad Range
393 Assay Kit (ThermoScientific).

394

395 **Library preparation for transposon directed insertion sequencing**

396 DNA (2 µg) was resuspended in 50 µL distilled water and sheared to approximately 550 bp
397 fragments using a S220 focussed-ultrasonicator (Covaris), according to the manufacturer's
398 protocol. Fragmented DNA was repaired using NEBNext blunt-end repair kit (New England
399 Biolabs) and purified using Monarch PCR clean-up kit (NEB). Blunted DNA was A-tailed using
400 NEBNext dA-tailing kit (NEB) and column purified. Custom transposon sequencing adaptors
401 (Supplementary Table S3) were generated by heating an equimolar mix of Com_AdaptorPt1
402 primer and Com_AdaptorPt2 (P7+index) primers to 95°C for 5 min, followed by cooling by
403 1°C every 40 s to a final temperature of 4°C in a thermocycler. Adaptors were ligated to A-
404 tailed library fragments using NEBNext quick ligase kit. Transposon-containing fragments
405 were enriched by PCR using ComP7 primer (10 µM) and an equimolar mix of primers P5-
406 IR2a-d primer (10 µM) in a reaction with 50 ng of adaptor ligated template and Phusion DNA

407 polymerase (NEB) in a thermocycler with the following program 98°C 3 min; 4 cycles of 98°C
408 20s, 70°C 20s, 72°C 1 min; 20 cycles of 98°C 20s, 67°C 20s, 72°C 1 min; 72°C 3 min.
409 Transposon-enriched libraries were subsequently purified with AMPureXP beads
410 (Beckman), pooled together and further purified using AMPure XP beads.

411

412 **Data analysis**

413 Indexed libraries were combined, spiked with 20% PhiX, and sequenced on the Illumina
414 Hiseq 3000 platform, using v2 chemistry, generating single-end reads of 250 bp. Raw .fastq
415 sequencing files were analysed for quality and pre-processed using the TRANSIT TPP tool
416 (75) set to default 'Sassetti' protocol, in order to remove transposon tags and adapter
417 sequences, and to map reads using BWA-mem to TA sites to the *M. bovis* AF2122/97
418 genome (NC_002945.3). The TRANSIT 'tnseq_stats' tool was run on each sample to assess
419 insertion density, skew, kurtosis and potential amplification bias.

420 The *M. bovis* AF2122/97 genome was scanned for the non-permissive Himar1
421 transposon insertion motif ('SGNTANCS', where S is either G or C and N is any base) as
422 previously described [10]. 6605 sites were identified as non-permissive (approximately 9%
423 of total TA sites) and excluded from resampling analysis. A custom annotation, '.prot-table'
424 for TRANSIT, was created from the *M. bovis* AF2122/97 annotation file (NCBI Accession
425 Number LT708304, version LT708304.1). TRANSIT HMM was run on the input library using
426 the default normalisation (TTR) with LOESS correction for genomic position bias. Each TA
427 site was assigned an essentiality state and genes were assigned an essentiality call based on
428 the assigned state of the TA sites within annotated gene boundaries.

429 Resampling between the input library and each of the output sample libraries was
430 performed independently using the TRANSIT resampling algorithm and the complete prot-
431 table. TTR normalisation was used for 23 of the samples, and betageom normalisation for
432 the three samples with skew of greater than 50. The initial resampling output files were
433 evaluated to identify genes with very few, or no, reads at any TA site within the gene
434 boundaries in both the input library and output sample libraries. Genes with no read counts
435 greater than 4 at any TA site, in any sample, and with a sum of all reads at any TA site across
436 the 26 samples less than 55, were flagged. Essential and unchanged genes were removed
437 from the prot-table prior to further evaluation. Resampling was further limited to protein-
438 coding genes. Resampling was re-run for each sample using the attenuated prot-table and
439 an edited TRANSIT resampling script to return the left-tail p-value, as the data were
440 expected to reflect attenuation. All p-values were corrected for multiple testing with FDR
441 adjustment.

442 All analysis and plots were performed using R and R packages, tidyverse and circlize
443 (76–78). Orthologous TB genes were obtained from supplementary data files published by
444 Malone et al, 2018 (27). All scripts, prot-tables and insertion files are available at
445 https://github.com/jenjane118/Mbovis_in-vivo_Tnseq, DOI:10.5281/zenodo.6354151.
446 Sequencing files (.fastq) are deposited in SRA (Bioproject ID: PRJNA816175, Submission ID:
447 SUB11067380)

448

449 **Funding**

450 This work was funded by the BBSRC Grant Ref: BB/N004590/1 [awarded to SK (PI), DW (Co-
451 I), BW (Co-I), and SE3314 to BV-R as part of the joint BBSRC-DEFRA EradbTB consortium. AG,

IP, and SW were supported by the funding. VF was in receipt of an RVC PhD studentship. AG currently holds a Sêr Cymru II Lectureship funded by the European Research Development Fund and Welsh Government. BV-R is a Ser Cymru II Professor of Immunology at Aberystwyth University. JS is supported by a Bloomsbury Colleges PhD Studentship (LIDo program).

AUTHOR CONTRIBUTIONS

SK, DW, BW, BV-R and SB undertook funding acquisition and designed the study. AJG, VF, JM, SW, IP, MC carried out the experimental work. Data analysis was done by IN and JS. AJG, JS and SLK wrote the first draft of the manuscript. All authors contributed to the manuscript revision, read, and approved the submitted version.

Acknowledgements

The authors would like to acknowledge the help and support of APHA colleagues from the BAC4 workgroup and the Pathology Unit, and in particular acknowledge the care and support provided to animals under experimentation by members of APHA's Animals Sciences Unit. We would like to thank Dr Dany Beste for useful discussions surrounding the role of *glpD2* in mycobacterial metabolism.

470 **References**

471 1. Müller B, Dürr S, Alonso S, Hattendorf J, Laisse CJM, Parsons SDC, van Helden PD,
472 Zinsstag J. 2013. Zoonotic Mycobacterium bovis-induced tuberculosis in humans.
473 Emerg Infect Dis 19:899–908.

474 2. Mableson HE, Okello A, Picozzi K, Welburn SC. 2014. Neglected Zoonotic Diseases—
475 The Long and Winding Road to Advocacy. PLoS Negl Trop Dis 8:e2800.

476 3. Bayissa B, Sirak A, Worku A, Zewude A, Zeleke Y, Chanyalew M, Gumi B, Berg S,
477 Conlan A, Hewinson RG, Wood JLN, Vordermeier HM, Ameni G. 2021. Evaluation of
478 the Efficacy of BCG in Protecting Against Contact Challenge With Bovine Tuberculosis
479 in Holstein-Friesian and Zebu Crossbred Calves in Ethiopia. Front Vet Sci 8.

480 4. Srinivasan S, Conlan AJK, Easterling LA, Herrera C, Dandapat P, Veerasami M, Ameni
481 G, Jindal N, Raj GD, Wood J, Juleff N, Bakker D, Vordermeier M, Kapur V. 2021. A
482 Meta-Analysis of the Effect of Bacillus Calmette-Guérin Vaccination Against Bovine
483 Tuberculosis: Is Perfect the Enemy of Good? Front Vet Sci 0:116.

484 5. Vordermeier HM, Whelan A, Cockle PJ, Farrant L, Palmer N, Hewinson RG. 2001. Use
485 of synthetic peptides derived from the antigens ESAT-6 and CFP-10 for differential
486 diagnosis of bovine tuberculosis in cattle. Clin Diagn Lab Immunol 8:571–578.

487 6. Whelan AO, Clifford D, Upadhyay B, Breadon EL, McNair J, Hewinson GR, Vordermeier
488 MH. 2010. Development of a skin test for bovine tuberculosis for differentiating
489 infected from vaccinated animals. J Clin Microbiol 48:3176–3181.

490 7. Cain AK, Barquist L, Goodman AL, Paulsen IT, Parkhill J, van Opijnen T. 2020. A decade
491 of advances in transposon-insertion sequencing. Nat Rev Genet. Nat Rev Genet.

492 8. Zhang YJ, Reddy MC, Ioerger TR, Rothchild AC, Dartois V, Schuster BM, Trauner A,
493 Wallis D, Galaviz S, Huttenhower C, Sacchettini JC, Behar SM, Rubin EJ. 2013.
494 Tryptophan biosynthesis protects mycobacteria from CD4 T-cell-mediated killing. Cell
495 155:1296–1308.

496 9. Bellerose MM, Proulx MK, Smith CM, Baker RE, Ioerger TR, Sassetti CM. 2020. Distinct
497 Bacterial Pathways Influence the Efficacy of Antibiotics against Mycobacterium
498 tuberculosis. mSystems 5.

499 10. Dejesus MA, Gerrick ER, Xu W, Park SW, Long JE, Boutte CC, Rubin EJ, Schnappinger D,
500 Ehrt S, Fortune SM, Sassetti CM, Ioerger TR. 2017. Comprehensive essentiality
501 analysis of the Mycobacterium tuberculosis genome via saturating transposon
502 mutagenesis. MBio 8.

503 11. Griffin JE, Gawronski JD, Dejesus MA, Ioerger TR, Akerley BJ, Sassetti CM. 2011. High-
504 resolution phenotypic profiling defines genes essential for mycobacterial growth and
505 cholesterol catabolism. PLoS Pathog 7:e1002251.

506 12. Patil S, Palande A, Lodhiya T, Pandit A, Mukherjee R. 2021. Redefining genetic
507 essentiality in Mycobacterium tuberculosis. Gene 765.

508 13. Sassetti CM, Rubin EJ. 2003. Genetic requirements for mycobacterial survival during
509 infection. Proc Natl Acad Sci U S A 100:12989–12994.

510 14. Rhijn I Van, Branch Moody D. CD1 and mycobacterial lipids activate human T cells
511 https://doi.org/10.1111/imr.12253.

512 15. Dutta NK, Mehra S, Didier PJ, Roy CJ, Doyle LA, Alvarez X, Ratterree M, Be NA,
513 Lamichhane G, Jain SK, Lacey MR, Lackner AA, Kaushal D. 2010. Genetic Requirements

514 for the Survival of Tubercle Bacilli in Primates. J Infect Dis 201:1743–1752.

515 16. Mendum TA, Chandran A, Williams K, Vordermeier HM, Villarreal-Ramos B, Wu H,
516 Singh A, Smith AA, Butler RE, Prasad A, Bharti N, Banerjee R, Kasibhatla SM, Bhatt A,
517 Stewart GR, McFadden J. 2019. Transposon libraries identify novel Mycobacterium
518 bovis BCG genes involved in the dynamic interactions required for BCG to persist
519 during in vivo passage in cattle. BMC Genomics 20:431.

520 17. Smith AA, Villarreal-Ramos B, Mendum TA, Williams KJ, Jones GJ, Wu H, McFadden J,
521 Vordermeier HM, Stewart GR. 2020. Genetic screening for the protective antigenic
522 targets of BCG vaccination. Tuberculosis 124:101979.

523 18. Gibson AJ, Passmore IJ, Faulkner V, Xia D, Nobeli I, Stiens J, Willcocks S, Clark TG,
524 Sobkowiak B, Werling D, Villarreal-Ramos B, Wren BW, Kendall SL. 2021. Probing
525 Differences in Gene Essentiality Between the Human and Animal Adapted Lineages of
526 the Mycobacterium tuberculosis Complex Using TnSeq. Front Vet Sci 8.

527 19. Majumdar G, Mbau R, Singh V, Warner DF, Dragset MS, Mukherjee R. 2017. Genome-
528 wide transposon mutagenesis in Mycobacterium tuberculosis and Mycobacterium
529 smegmatis, p. 321–335. *In* Methods in Molecular Biology. Humana Press, New York,
530 NY.

531 20. Lewis KN, Liao R, Guinn KM, Hickey MJ, Smith S, Behr MA, Sherman DR. 2003.
532 Deletion of RD1 from Mycobacterium tuberculosis Mimics Bacille Calmette-Guérin
533 Attenuation . J Infect Dis 187:117–123.

534 21. Phan TH, van Leeuwen LM, Kuijl C, Ummels R, van Stempvoort G, Rubio-Canalejas A,
535 Piersma SR, Jiménez CR, van der Sar AM, Houben ENG, Bitter W. 2018. EspH is a

536 hypervirulence factor for Mycobacterium marinum and essential for the secretion of
537 the ESX-1 substrates EspE and EspF. PLoS Pathog 14:e1007247.

538 22. Inwald J, Jahans K, Hewinson RG, Gordon S V. 2003. Inactivation of the
539 Mycobacterium bovis homologue of the polymorphic RD1 gene Rv3879c (Mb3909c)
540 does not affect virulence. Tuberculosis (Edinb) 83:387–393.

541 23. Bold TD, Davis DC, Penberthy KK, Cox LM, Ernst JD, de Jong BC. 2012. Impaired fitness
542 of Mycobacterium africanum despite secretion of ESAT-6. J Infect Dis 205:984–90.

543 24. Hotter GS, Wards BJ, Mouat P, Besra GS, Gomes J, Singh M, Bassett S, Kawakami P,
544 Wheeler PR, De Lisle GW, Collins DM. 2005. Transposon mutagenesis of Mb0100 at
545 the ppe1-nrp locus in Mycobacterium bovis disrupts phthiocerol dimycocerosate
546 (PDIM) and glycosylphenol-PDIM biosynthesis, producing an avirulent strain with
547 vaccine properties at least equal to those of M. bovis BCG. J Bacteriol 187:2267–2277.

548 25. Cox JS, Chess B, McNeil M, Jacobs WR. 1999. Complex lipid determines tissue-specific
549 replication of Mycobacterium tuberculosis in mice. Nature 402:79–83.

550 26. Pérez J, Garcia R, Bach H, de Waard JH, Jacobs WR, Av-Gay Y, Bubis J, Takiff HE. 2006.
551 Mycobacterium tuberculosis transporter MmpL7 is a potential substrate for kinase
552 PknD. Biochem Biophys Res Commun 348:6–12.

553 27. Malone KM, Rue-Albrecht K, Magee DA, Conlon K, Schubert OT, Nalpas NC, Browne
554 JA, Smyth A, Gormley E, Aebersold R, Machugh DE, Gordon S V. 2018. Comparative
555 ’omics analyses differentiate mycobacterium tuberculosis and mycobacterium bovis
556 and reveal distinct macrophage responses to infection with the human and bovine
557 tubercle bacilli. Microb Genomics 4.

558 28. Pisu D, Huang L, Grenier JK, Russell DG. 2020. Dual RNA-Seq of Mtb-Infected
559 Macrophages In Vivo Reveals Ontologically Distinct Host-Pathogen Interactions. Cell
560 Rep 30:335-350.e4.

561 29. Van Der Geize R, Yam K, Heuser T, Wilbrink MH, Hara H, Anderton MC, Sim E,
562 Dijkhuizen L, Davies JE, Mohn WW, Eltis LD. 2007. A gene cluster encoding cholesterol
563 catabolism in a soil actinomycete provides insight into Mycobacterium tuberculosis
564 survival in macrophages. Proc Natl Acad Sci U S A 104:1947–1952.

565 30. Nesbitt NM, Yang X, Fontán P, Kolesnikova I, Smith I, Sampson NS, Dubnau E. 2010. A
566 thiolase of Mycobacterium tuberculosis is required for virulence and production of
567 androstenedione and androstadienedione from cholesterol. Infect Immun 78:275–
568 282.

569 31. Bandyopadhyay U, Chadha A, Gupta P, Tiwari B, Bhattacharyya K, Popli S, Raman R,
570 Brahamachari V, Singh Y, Malhotra P, Natarajan K. 2017. Suppression of Toll-like
571 receptor 2-mediated proinflammatory responses by Mycobacterium tuberculosis
572 protein Rv3529c. J Leukoc Biol 102:1249–1259.

573 32. Pandey AK, Sassetti CM. 2008. Mycobacterial persistence requires the utilization of
574 host cholesterol. Proc Natl Acad Sci U S A 105:4376–4380.

575 33. Mohn WW, Van Der Geize R, Stewart GR, Okamoto S, Liu J, Dijkhuizen L, Eltis LD.
576 2008. The actinobacterial mce4 locus encodes a steroid transporter. J Biol Chem
577 283:35368–35374.

578 34. Lee W, VanderVen BC, Fahey RJ, Russell DG. 2013. Intracellular Mycobacterium
579 tuberculosis exploits host-derived fatty acids to limit metabolic stress. J Biol Chem

580 288:6788–6800.

581 35. Jain M, Petzold CJ, Schelle MW, Leavell MD, Mougous JD, Bertozzi CR, Leary JA, Cox
582 JS. 2007. Lipidomics reveals control of Mycobacterium tuberculosis virulence lipids via
583 metabolic coupling. Proc Natl Acad Sci U S A 104:5133.

584 36. Singh P, Sinha R, Tyagi G, Sharma NK, Saini NK, Chandolia A, Prasad AK, Varma-Basil
585 M, Bose M. 2018. PDIM and SL1 accumulation in Mycobacterium tuberculosis is
586 associated with mce4A expression. Gene 642:178–187.

587 37. Yang X, Gao J, Smith I, Dubnau E, Sampson NS. 2011. Cholesterol Is Not an Essential
588 Source of Nutrition for Mycobacterium tuberculosis during Infection. J Bacteriol
589 193:1473.

590 38. Ouellet H, Guan S, Johnston JB, Chow ED, Kells PM, Burlingame AL, Cox JS, Podust LM,
591 De Montellano PRO. 2010. Mycobacterium tuberculosis CYP125A1, a steroid C27
592 monooxygenase that detoxifies intracellularly generated cholest-4-en-3-one. Mol
593 Microbiol 77:730–742.

594 39. Serafini A, Tan L, Horswell S, Howell S, Greenwood DJ, Hunt DM, Phan MD, Schembri
595 M, Monteleone M, Montague CR, Britton W, Garza-Garcia A, Snijders AP, VanderVen
596 B, Gutierrez MG, West NP, de Carvalho LPS. 2019. Mycobacterium tuberculosis
597 requires glyoxylate shunt and reverse methylcitrate cycle for lactate and pyruvate
598 metabolism. Mol Microbiol 112:1284–1307.

599 40. Safi H, Gopal P, Lingaraju S, Ma S, Levine C, Dartois V, Yee M, Li L, Blanc L, Liang HPH,
600 Husain S, Hoque M, Soteropoulos P, Rustad T, Sherman DR, Dick T, Alland D. 2019.
601 Phase variation in Mycobacterium tuberculosis glpK produces transiently heritable

602 drug tolerance. Proc Natl Acad Sci U S A 116:19665–19674.

603 41. De Carvalho LPS, Fischer SM, Marrero J, Nathan C, Ehrt S, Rhee KY. 2010.
604 Metabolomics of Mycobacterium tuberculosis Reveals Compartmentalized Co-
605 Catabolism of Carbon Substrates. Chem Biol 17:1122–1131.

606 42. Carroll P, Parish T. 2015. Deletion of cyp125 Confers Increased Sensitivity to Azoles in
607 Mycobacterium tuberculosis. PLoS One 10:e0133129.

608 43. Borah K, Mendum TA, Hawkins ND, Ward JL, Beale MH, Larrouy-Maumus G, Bhatt A,
609 Moulin M, Haertlein M, Strohmeier G, Pichler H, Forsyth VT, Noack S, Goulding CW,
610 McFadden J, Beste DJ V. 2021. Metabolic fluxes for nutritional flexibility of
611 Mycobacterium tuberculosis. Mol Syst Biol 17.

612 44. Keating LA, Wheeler PR, Mansoor H, Inwald JK, Dale J, Hewinson RG, Gordon S V.
613 2005. The pyruvate requirement of some members of the Mycobacterium
614 tuberculosis complex is due to an inactive pyruvate kinase: implications for in vivo
615 growth. Mol Microbiol 56:163–174.

616 45. Lofthouse EK, Wheeler PR, Beste DJV, Khatri BL, Wu H, Mendum TA, Kierzek AM,
617 McFadden J. 2013. Systems-based approaches to probing metabolic variation within
618 the Mycobacterium tuberculosis complex. PLoS One 8.

619 46. Chandra P, Coullon H, Agarwal M, Goss CW, Philips JA. 2022. Macrophage global
620 metabolomics identifies cholestenone as host/pathogen cometabolite present in
621 human Mycobacterium tuberculosis infection. J Clin Invest 132.

622 47. Golby P, Hatch KA, Bacon J, Cooney R, Riley P, Allnutt J, Hinds J, Nunez J, Marsh PD,
623 Hewinson RG, Gordon S V. 2007. Comparative transcriptomics reveals key gene

624 expression differences between the human and bovine pathogens of the
625 Mycobacterium tuberculosis complex. Microbiology 153:3323–3336.

626 48. Rehren G, Walters S, Fontan P, Smith I, Zárraga AM. 2007. Differential gene
627 expression between Mycobacterium bovis and Mycobacterium tuberculosis.
628 Tuberculosis (Edinb) 87:347–359.

629 49. Gonzalo-Asensio J, Malaga W, Pawlik A, Astarie-Dequeker C, Passemar C, Moreau F,
630 Laval F, Daffé M, Martin C, Brosch R, Guilhot C. 2014. Evolutionary history of
631 tuberculosis shaped by conserved mutations in the PhoPR virulence regulator. Proc
632 Natl Acad Sci U S A 111:11491–11496.

633 50. White AD, Sibley L, Sarfas C, Morrison A, Gullick J, Clark S, Gleeson F, McIntyre A,
634 Arlehamn CL, Sette A, Salguero FJ, Rayner E, Rodriguez E, Puentes E, Laddy D,
635 Williams A, Dennis M, Martin C, Sharpe S. 2021. MTBVAC vaccination protects rhesus
636 macaques against aerosol challenge with M. tuberculosis and induces immune
637 signatures analogous to those observed in clinical studies. NPJ Vaccines 6.

638 51. Gonzalo-Asensio J, Marinova D, Martin C, Aguilo N. 2017. MTBVAC: Attenuating the
639 Human Pathogen of Tuberculosis (TB) Toward a Promising Vaccine against the TB
640 Epidemic. Front Immunol 8:1803.

641 52. Altes HK, Dijkstra F, Lugnèr A, Cobelens F, Wallinga J. 2009. Targeted bcg vaccination
642 against severe tuberculosis in low-prevalence settings epidemiologic and economic
643 assessment. Epidemiology 20:562–568.

644 53. Frigui W, Bottai D, Majlessi L, Monot M, Josselin E, Brodin P, Garnier T, Gicquel B,
645 Martin C, Leclerc C, Cole ST, Brosch R. 2008. Control of M. tuberculosis ESAT-6

646 secretion and specific T cell recognition by PhoP. PLoS Pathog 4.

647 54. Pang X, Samten B, Cao G, Wang X, Tvinnereim AR, Chen XL, Howard ST. 2013. MprAB
648 regulates the espA operon in Mycobacterium tuberculosis and modulates ESX-1
649 function and host cytokine response. J Bacteriol 195:66–75.

650 55. Queval CJ, Fearns A, Botella L, Smyth A, Schnettger L, Mitermite M, Wooff E,
651 Villarreal-Ramos B, Garcia-Jimenezi W, Heunis T, Trosti M, Werlingi D, Salguero FJ,
652 Gordon S V., Gutierrez MG. 2021. Macrophage-specific responses to human- and
653 animal-adapted tubercle bacilli reveal pathogen and host factors driving
654 multinucleated cell formation. PLoS Pathog 17.

655 56. Churchill GA, Airey DC, Allayee H, Angel JM, Attie AD, Beatty J, Beavis WD, Belknap JK,
656 Bennett B, Berrettini W, Bleich A, Bogue M, Broman KW, Buck KJ, Buckler E,
657 Burmeister M, Chesler EJ, Cheverud JM, Clapcote S, Cook MN, Cox RD, Crabbe JC,
658 Crusio WE, Darvasi A, Deschepper CF, Doerge RW, Farber CR, Forejt J, Gaile D, Garlow
659 SJ, Geiger H, Gershenfeld H, Gordon T, Gu J, Gu W, de Haan G, Hayes NL, Heller C,
660 Himmelbauer H, Hitzemann R, Hunter K, Hsu HC, Iraqi FA, Ivandic B, Jacob HJ, Jansen
661 RC, Jepsen KJ, Johnson DK, Johnson TE, Kempermann G, Kendziorski C, Kotb M, Kooy
662 RF, Llamas B, Lammert F, Lassalle JM, Lowenstein PR, Lu L, Lusis A, Manly KF,
663 Marcucio R, Matthews D, Medrano JF, Miller DR, Mittleman G, Mock BA, Mogil JS,
664 Montagutelli X, Morahan G, Morris DG, Mott R, Nadeau JH, Nagase H, Nowakowski
665 RS, O'Hara BF, Osadchuk A V., Page GP, Paigen B, Paigen K, Palmer AA, Pan HJ,
666 Peltonen-Palotie L, Peirce J, Pomp D, Pravenec M, Prows DR, Qi Z, Reeves RH, Roder J,
667 Rosen GD, Schadt EE, Schalkwyk LC, Seltzer Z, Shimomura K, Shou S, Sillanpää MJ,
668 Siracusa LD, Snoeck HW, Spearow JL, Svenson K, Tarantino LM, Threadgill D, Toth LA,

669 Valdar W, Pardo-Manuel de Villena F, Warden C, Whatley S, Williams RW, Wiltshire T,
670 Yi N, Zhang D, Zhang M, Zou F. 2004. The Collaborative Cross, a community resource
671 for the genetic analysis of complex traits. Nat Genet 2004 3611 36:1133–1137.

672 57. Smith CM, Baker RE, Proulx MK, Mishra BB, Long JE, Park SW, Lee H-N, Kiritsy MC,
673 Bellerose MM, Olive AJ, Murphy KC, Papavinasasundaram K, Boehm FJ, Reames CJ,
674 Meade RK, Hampton BK, Linnertz CL, Shaw GD, Hock P, Bell TA, Ehrt S, Schnappinger
675 D, Pardo-Manuel de Villena F, Ferris MT, Ioerger TR, Sassetti CM. 2022. Host-
676 pathogen genetic interactions underlie tuberculosis susceptibility in genetically
677 diverse mice. Elife 11.

678 58. Cowley S, Ko M, Pick N, Chow R, Downing KJ, Gordhan BG, Betts JC, Mizrahi V, Smith
679 DA, Stokes RW, Av-Gay Y. 2004. The Mycobacterium tuberculosis protein
680 serine/threonine kinase PknG is linked to cellular glutamate/glutamine levels and is
681 important for growth in vivo. Mol Microbiol 52:1691–1702.

682 59. Liu CF, Tonini L, Malaga W, Beau M, Stella A, Bouyssié D, Jackson MC, Nigou J, Puzo G,
683 Guilhot C, Burlet-Schiltz O, Rivière M. 2013. Bacterial protein-O-mannosylating
684 enzyme is crucial for virulence of Mycobacterium tuberculosis. Proc Natl Acad Sci U S
685 A 110:6560–6565.

686 60. Maksymiuk C, Balakrishnan A, Bryk R, Rhee KY, Nathan CF. 2015. E1 of?-
687 ketoglutarate dehydrogenase defends Mycobacterium tuberculosis against glutamate
688 anaplerosis and nitroxidative stress. Proc Natl Acad Sci U S A 112:E5834–E5843.

689 61. Venugopal A, Bryk R, Shi S, Rhee K, Rath P, Schnappinger D, Ehrt S, Nathan C. 2011.
690 Virulence of Mycobacterium tuberculosis depends on lipoamide dehydrogenase, a

691 member of three multienzyme complexes. Cell Host Microbe 9:21–31.

692 62. Constant P, Perez E, Malaga W, Lanéelle MA, Saurel O, Daffé M, Guilhot C. 2002. Role
693 of the pks15/1 Gene in the Biosynthesis of Phenolglycolipids in the Mycobacterium
694 tuberculosisComplex: EVIDENCE THAT ALL STRAINS SYNTHESIZE GLYCOSYLATEDp-
695 HYDROXYBENZOIC METHYL ESTERS AND THAT STRAINS DEVOID OF
696 PHENOLGLYCOLIPIDS HARBOR A FRAMESHIFT MU. J Biol Chem 277:38148–38158.

697 63. Samanta S, Singh A, Biswas P, Bhatt A, Visweswariah SS. 2017. Mycobacterial phenolic
698 glycolipid synthesis is regulated by cAMP-dependent lysine acylation of FadD22.
699 Microbiol (United Kingdom) 163:373–382.

700 64. Yang S, Sui S, Qin Y, Chen H, Sha S, Liu X, Deng G, Ma Y. 2022. Protein O-
701 mannosyltransferase Rv1002c contributes to low cell permeability, biofilm formation
702 in vitro, and mycobacterial survival in mice. APMIS 130:181–192.

703 65. Crellin PK, Kovacevic S, Martin KL, Brammananth R, Morita YS, Billman-Jacobe H,
704 McConville MJ, Coppel RL. 2008. Mutations in pimE restore lipoarabinomannan
705 synthesis and growth in a Mycobacterium smegmatis lpqW mutant. J Bacteriol
706 190:3690–3699.

707 66. Butler RE, Smith AA, Mendum TA, Chandran A, Wu H, Lefrançois L, Chambers M,
708 Soldati T, Stewart GR. 2020. Mycobacterium bovis uses the ESX-1 Type VII secretion
709 system to escape predation by the soil-dwelling amoeba Dictyostelium discoideum.
710 ISME J 14:919.

711 67. Agapova A, Serafini A, Petridis M, Hunt DM, Garza-Garcia A, Sohaskey CD, de Carvalho
712 LPS. 2019. Flexible nitrogen utilisation by the metabolic generalist pathogen

713 Mycobacterium tuberculosis. Elife 8.

714 68. Yeh JI, Chinte U, Du S. 2008. Structure of glycerol-3-phosphate dehydrogenase, an
715 essential monotopic membrane enzyme involved in respiration and metabolism. Proc
716 Natl Acad Sci U S A 105:3280.

717 69. Cook GM, Hards K, Dunn E, Heikal A, Nakatani Y, Greening C, Crick DC, Fontes FL,
718 Pethe K, Hasenoehrl E, Berney M. 2017. Drug Discovery & Development: State-of-the-
719 Art and Future Directions" on the topic of "Targets": OXPHOS as a target space for
720 tuberculosis: success, caution, and future directions. Microbiol Spectr 5.

721 70. Bald D, Villellas C, Lu P, Koul A. 2017. Targeting energy metabolism in Mycobacterium
722 tuberculosis, a new paradigm in antimycobacterial drug discovery. MBio 8.

723 71. Garnier T, Eiglmeier K, Camus J-C, Medina N, Mansoor H, Pryor M, Duthoy S, Grondin
724 S, Lacroix C, Monsempe C, Simon S, Harris B, Atkin R, Doggett J, Mayes R, Keating L,
725 Wheeler PR, Parkhill J, Barrell BG, Cole ST, Gordon S V., Hewinson RG. 2003. The
726 complete genome sequence of Mycobacterium bovis. Proc Natl Acad Sci U S A
727 100:7877.

728 72. Larrouy-Maumus G, Biswas T, Hunt DM, Kelly G, Tsodikov O V., De Carvalho LPS.
729 2013. Discovery of a glycerol 3-phosphate phosphatase reveals glycerophospholipid
730 polar head recycling in Mycobacterium tuberculosis. Proc Natl Acad Sci U S A
731 110:11320–11325.

732 73. Gallagher J, Horwill DM. 1977. A selective oleic acid albumin agar medium for the
733 cultivation of Mycobacterium bovis. J Hyg (Lond) 79:155.

734 74. Vordermeier HM, Chambers MA, Cockle PJ, Whelan AO, Simmons J, Hewinson RG.

735 2002. Correlation of ESAT-6-specific gamma interferon production with pathology in
736 cattle following Mycobacterium bovis BCG vaccination against experimental bovine
737 tuberculosis. Infect Immun 70:3026–3032.

738 75. DeJesus MA, Ambadipudi C, Baker R, Sassetti C, Ioerger TR. 2015. TRANSIT--A
739 Software Tool for Himar1 TnSeq Analysis. PLoS Comput Biol 11.

740 76. Gu Z, Gu L, Eils R, Schlesner M, Brors B. 2014. circlize Implements and enhances
741 circular visualization in R. Bioinformatics 30:2811–2812.

742 77. R Core Team. R: A Language and Environment for Statistical Computing.

743 78. Wickham H, Averick M, Bryan J, Chang W, D' L, Mcgowan A, François R, Grolemund G,
744 Hayes A, Henry L, Hester J, Kuhn M, Lin Pedersen T, Miller E, Bache SM, Müller K,
745 Ooms J, Robinson D, Seidel DP, Spinu V, Takahashi K, Vaughan D, Wilke C, Woo K,
746 Yutani H. 2019. Welcome to the Tidyverse. J Open Source Softw 4:1686.

747

748

749 **Figure Legends**

750 **Figure 1. bTB specific IFN-gamma release in cattle infected with the *M. bovis* Tn-library.**
751 Blood was collected from all 24 animals on the day of infection and 2 weeks later. No
752 response was detected to either PPD-A or PPD-B antigen stimulation prior to infection
753 (Figure 1A and Figure 1B, week 0). All animals presented a significant and specific response
754 to PPD-B compared to PPD-A as determined by a paired T-test using GraphPad Prism (Figure
755 1C). *** $p \leq 0.001$

756

757 **Figure 2. Tissue pathology and bacterial load in tissue sites. Six weeks after infection**
758 **animals were subjected to post-mortem examination.** Gross pathology and evidence of TB-
759 like granulomas lesions were scored. Data presented is the mean across animals of the total
760 scores for each tissue group from 24 animals +/- the standard deviation. Lung and thoracic
761 lymph nodes were observed to contain the highest pathology compared to head and neck
762 lymph nodes (Figure 2A). For bacterial load estimation, aliquots of macerates were plated
763 onto modified 7H11 agar containing kanamycin. Colonies were counted after 3-4 weeks
764 growth. Data are presented as mean CFU/ml per collected tissue group +/- standard
765 deviation. Lung tissue contained the highest bacterial burden compared to thoracic and
766 head and neck lymph nodes as determined by one-way ANOVA analysis using GraphPad
767 Prism (Figure 2b). *** $p \leq 0.001$, ** $p = 0.002$, *$p=0.01$

768

769 **Figure 3. Fold-changes caused by transposon insertions in the ESX-1 secretion system in**
770 **the lungs and lymph nodes of infected cattle.** Asterisks indicate that genes had an adjusted

771 p-value of <0.05 in at least half of the animals. The genes are grouped according to function
772 as indicated by the colour scheme. The log_2 fold-change are indicated on a yellow to red
773 scale and present as a dot in the centre of the gene.

774

775 **Figure 4. Violin plot of normalised log_2 fold changes in gene insertions recovered from**
776 **bovine lung or thoracic lymph node tissue samples in selected gene groups.** Black bars
777 indicate overall median of normalized log_2 fold-change among genes in grouping. White bars
778 indicate mean log_2 fold-change for each gene in the group across all samples in either lung
779 or lymph node tissue

780

781 **Figure 5. Comparison of reported log_2 fold-change in *M. bovis*, *M. bovis* BCG and Mtb**
782 **transposon insertion sequencing experiments for orthologous genes in the cholesterol**
783 **catabolic pathway.** Greatest attenuation (most negative log_2 fold-change) is coloured by
784 darkest red. Studies used for comparison include Mendum et al., (24) and Bellarose et al.,
785 (9). Grey bars represent genes for which there is no information as they were either ES or
786 GD in input library or had less than 5 insertions in any TA site in any sample (input and all
787 output).

788

789 **Figure 6. Fold-changes caused by transposon insertions in *phoP, phoR* and *fadD26* in the**
790 **lungs and lymph nodes of infected cattle.** Samples with adjusted p-values (BH-fdr
791 corrected) < 0.05 are indicated with purple points.

792

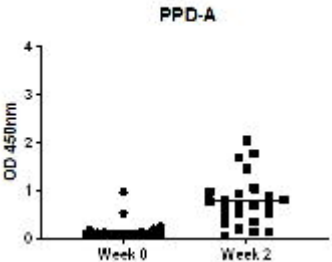
PPD-A
OD 450nm
4
3
2
1
0
Week 0
Week 2

(A)

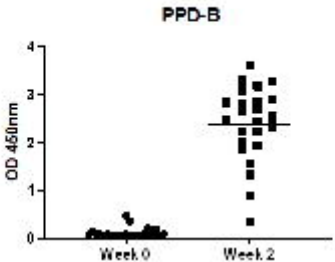
PPD-B
OD 450nm
4
3
2
1
0
Week 0
Week 2

(B)

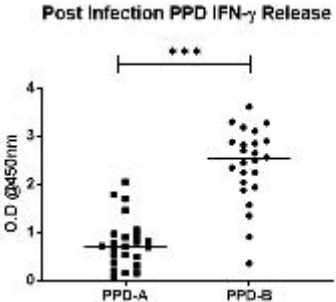
Post Infection PPD IFN-γ Release
***
O.D @450nm
4
3
2
1
0
PPD-A
PPD-B

(C)

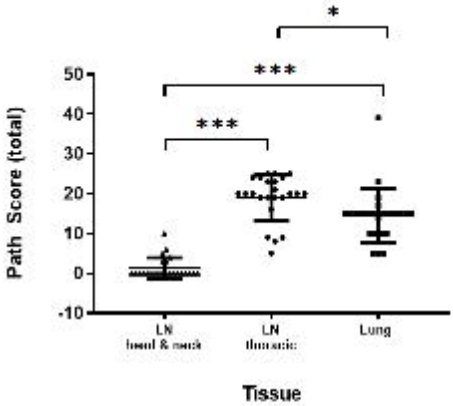
*
***
***
Path Score (total)
50
40
30
20
10
0
-10
LN
head & neck
LN
thoracic
Lung
Tissue

(A)

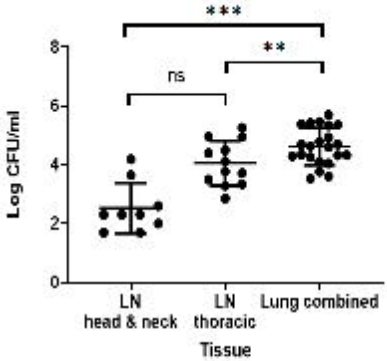
***
**
ns
Log CFU/ml
8
6
4
2
0
LN
head & neck
LN
thoracic
Lung combined
Tissue

(B)

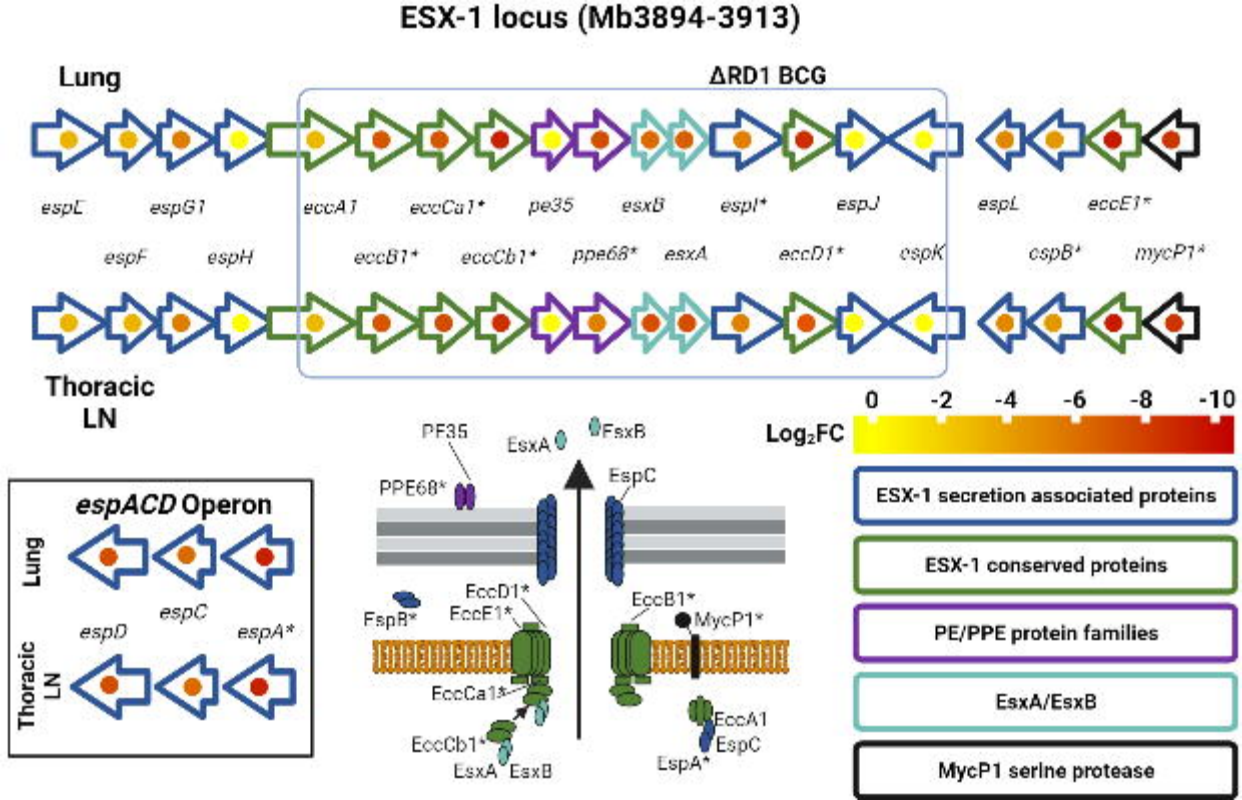
ESX-1 locus (Mb3894-3913)
Lung
ΔRD1 BCG
espE
espG1
eccA1
eccCa1*
pe35
esxB
espI*
espJ
espL
eccE1*
espF
espH
eccB1*
eccCb1*
ppe68*
esxA
eccD1*
espK
espB*
mycP1*
Thoracic LN
0
-2
-4
-6
-8
-10
Log2FC
espACD Operon
Lung
espC
espD
espA*
Thoracic LN
PE35
EsxA
EsxB
PPE68*
EspC
EspB*
EccD1*
EccE1*
EccB1*
MycP1*
EccCa1*
EccCb1*
EsxA
EsxB
EccA1
EspC
EspA*
ESX-1 secretion associated proteins
ESX-1 conserved proteins
PE/PPE protein families
EsxA/EsxB
MycP1 serine protease

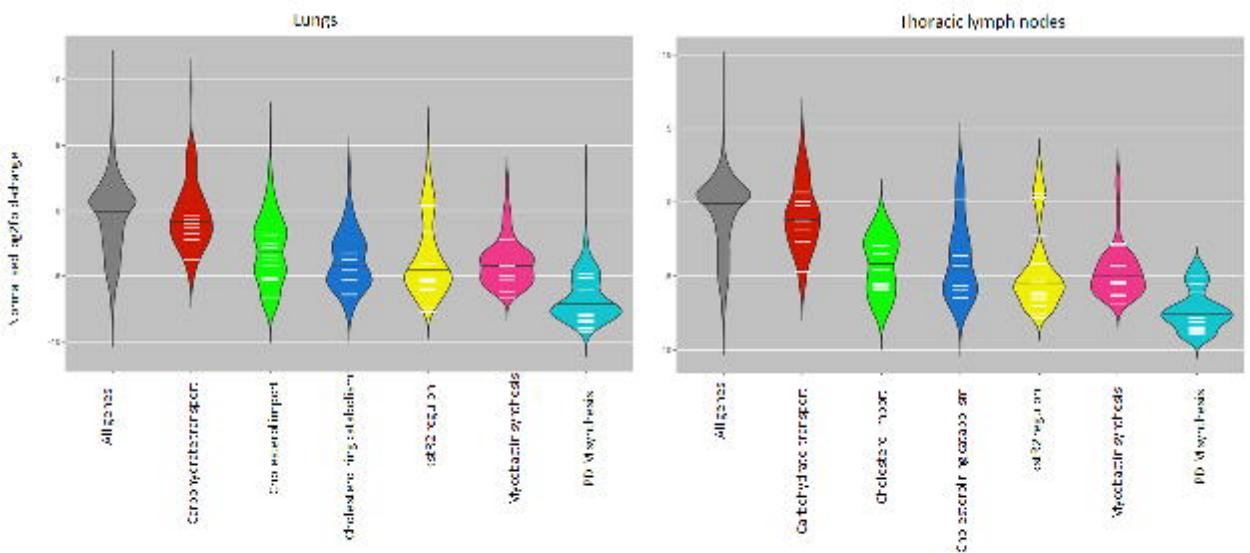
Lungs
Thoracic lymph nodes

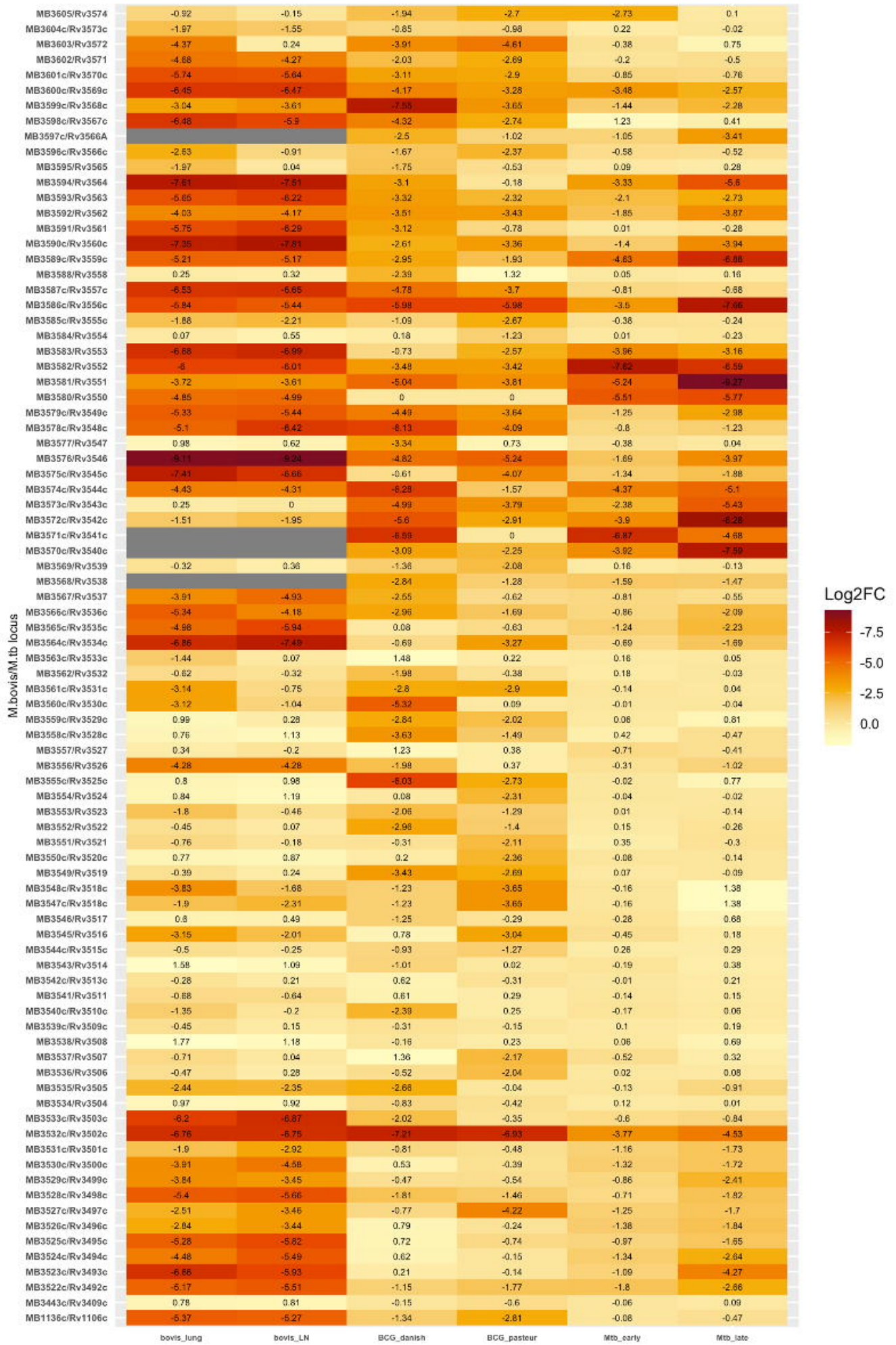
M.bovis/M.tb locus
MB3605/Rv3574 -0.92 -0.15 -1.94 -2.7 -2.73 0.1
MB3604c/Rv3573c -1.97 -1.55 -0.85 -0.98 0.22 -0.02
MB3603/Rv3572 -4.37 0.24 -3.91 -4.61 -0.38 0.75
MB3602/Rv3571 -4.88 -4.27 -2.03 -2.69 -0.2 -0.5
MB3601c/Rv3570c -5.74 -5.64 -3.11 -2.9 -0.85 -0.78
MB3600c/Rv3569c -6.45 -6.47 -4.17 -3.28 -3.48 -2.57
MB3599c/Rv3568c -3.04 -3.61 -7.55 -3.65 -1.44 -2.28
MB3598c/Rv3567c -6.48 -5.9 -4.32 -2.74 1.23 0.41
MB3597c/Rv3566A -2.5 -1.02 -1.05 -3.41
MB3596c/Rv3566c -2.63 -0.91 -1.67 -2.37 -0.58 -0.52
MB3595/Rv3565 -1.97 0.04 -1.75 -0.53 0.09 0.28
MB3594/Rv3564 -7.61 -7.51 -3.1 -0.18 -3.33 -5.6
MB3593/Rv3563 -5.65 -6.22 -3.32 -2.32 -2.1 -2.73
MB3592/Rv3562 -4.03 -4.17 -3.51 -3.43 -1.85 -3.87
MB3591/Rv3561 -5.75 -6.29 -3.12 -0.78 0.01 -0.28
MB3590c/Rv3560c -7.35 -7.81 -2.61 -3.36 -1.4 -3.94
MB3589c/Rv3559c -5.21 -5.17 -2.95 -1.93 -4.63 -6.88
MB3588/Rv3558 0.25 0.32 -2.39 1.32 0.05 0.16
MB3587c/Rv3557c -6.53 -6.65 -4.78 -3.7 -0.81 -0.68
MB3586c/Rv3556c -5.84 -5.44 -5.98 -5.98 -3.5 -7.66
MB3585c/Rv3555c -1.88 -2.21 -1.09 -2.67 -0.38 -0.24
MB3584/Rv3554 0.07 0.55 0.18 -1.23 0.01 -0.23
MB3583/Rv3553 -6.88 -6.99 -0.73 -2.57 -3.96 -3.16
MB3582/Rv3552 -6 -6.01 -3.48 -3.42 -7.62 -6.59
MB3581/Rv3551 -3.72 -3.61 -5.04 -3.81 -5.24 -9.27
MB3580/Rv3550 -4.85 -4.99 0 0 -5.51 -5.77
MB3579c/Rv3549c -5.33 -5.44 -4.49 -3.64 -1.25 -2.98
MB3578c/Rv3548c -5.1 -6.42 -6.13 -4.09 -0.8 -1.23
MB3577/Rv3547 0.98 0.62 -3.34 0.73 -0.38 0.04
MB3576/Rv3546 -9.11 -9.24 -4.82 -5.24 -1.69 -3.97
MB3575c/Rv3545c -7.41 -6.66 -0.61 -4.07 -1.34 -1.88
MB3574c/Rv3544c -4.43 -4.31 -6.28 -1.57 -4.37 -5.1
MB3573c/Rv3543c 0.25 0 -4.99 -3.79 -2.38 -5.43
MB3572c/Rv3542c -1.51 -1.95 -5.6 -2.91 -3.9 -6.28
MB3571c/Rv3541c -6.59 0 -6.87 -4.68
MB3570c/Rv3540c -3.09 -2.25 -3.92 -7.59
MB3569/Rv3539 -0.32 0.36 -1.36 -2.08 0.16 -0.13
MB3568/Rv3538 -2.84 -1.28 -1.59 -1.47
MB3567/Rv3537 -3.91 -4.93 -2.55 -0.62 -0.81 -0.55
MB3566c/Rv3536c -5.34 -4.18 -2.96 -1.69 -0.86 -2.09
MB3565c/Rv3535c -4.98 -5.94 0.08 -0.63 -1.24 -2.23
MB3564c/Rv3534c -6.86 -7.49 -0.69 -3.27 -0.69 -1.69
MB3563c/Rv3533c -1.44 0.07 1.48 0.22 0.16 0.05
MB3562/Rv3532 -0.62 -0.32 -1.98 -0.38 0.18 -0.03
MB3561c/Rv3531c -3.14 -0.75 -2.8 -2.9 -0.14 0.04
MB3560c/Rv3530c -3.12 -1.04 -5.32 0.09 -0.01 -0.04
MB3559c/Rv3529c 0.99 0.28 -2.84 -2.02 0.06 0.81
MB3558c/Rv3528c 0.76 1.13 -3.63 -1.49 0.42 -0.47
MB3557/Rv3527 0.34 -0.2 1.23 0.38 -0.71 -0.41
MB3556/Rv3526 -4.28 -4.28 -1.99 0.37 -0.31 -1.02
MB3555c/Rv3525c 0.8 0.98 -6.03 -2.73 -0.02 0.77
MB3554/Rv3524 0.84 1.19 0.08 -2.31 -0.04 -0.02
MB3553/Rv3523 -1.8 -0.46 -2.06 -1.29 0.01 -0.14
MB3552/Rv3522 -0.45 0.07 -2.98 -1.4 0.15 -0.26
MB3551/Rv3521 -0.76 -0.18 -0.31 -2.11 0.35 -0.3
MB3550c/Rv3520c 0.77 0.87 0.2 -2.36 -0.08 -0.14
MB3549/Rv3519 -0.39 0.24 -3.43 -2.69 0.07 -0.09
MB3548c/Rv3518c -3.83 -1.68 -1.23 -3.65 -0.16 1.38
MB3547c/Rv3518c -1.9 -2.31 -1.23 -3.65 -0.16 1.38
MB3546/Rv3517 0.8 0.49 -1.25 -0.29 -0.28 0.68
MB3545/Rv3516 -3.15 -2.01 0.78 -3.04 -0.45 0.18
MB3544c/Rv3515c -0.5 -0.25 -0.93 -1.27 0.26 0.29
MB3543/Rv3514 1.58 1.09 -1.01 0.02 -0.19 0.38
MB3542c/Rv3513c -0.28 0.21 0.62 -0.31 -0.01 0.21
MB3541/Rv3511 -0.68 -0.64 0.61 0.29 -0.14 0.15
MB3540c/Rv3510c -1.35 -0.2 -2.38 0.25 -0.17 0.06
MB3539c/Rv3509c -0.45 0.15 -0.31 -0.15 0.1 0.19
MB3538/Rv3508 1.77 1.18 -0.16 0.23 0.06 0.69
MB3537/Rv3507 -0.71 0.04 1.36 -2.17 -0.52 0.32
MB3536/Rv3506 -0.47 0.28 -0.52 -2.04 0.02 0.08
MB3535/Rv3505 -2.44 -2.35 -2.66 -0.04 -0.13 -0.91
MB3534/Rv3504 0.97 0.92 -0.83 -0.42 0.12 0.01
MB3533c/Rv3503c -6.2 -6.87 -2.02 -0.35 -0.6 -0.84
MB3532c/Rv3502c -6.76 -6.75 -7.21 -6.93 -3.77 -4.53
MB3531c/Rv3501c -1.9 -2.92 -0.81 -0.48 -1.16 -1.73
MB3530c/Rv3500c -3.91 -4.58 0.53 -0.39 -1.32 -1.72
MB3529c/Rv3499c -3.84 -3.45 -0.47 -0.54 -0.86 -2.41
MB3528c/Rv3498c -5.4 -5.66 -1.81 -1.46 -0.71 -1.82
MB3527c/Rv3497c -2.51 -3.46 -0.77 -4.22 -1.25 -1.7
MB3526c/Rv3496c -2.84 -3.44 0.79 -0.24 -1.38 -1.84
MB3525c/Rv3495c -5.28 -5.82 0.72 -0.74 -0.97 -1.65
MB3524c/Rv3494c -4.48 -5.49 0.62 -0.15 -1.34 -2.84
MB3523c/Rv3493c -6.66 -5.93 0.21 -0.14 -1.09 -4.27
MB3522c/Rv3492c -5.17 -5.51 -1.15 -1.77 -1.8 -2.66
MB3443c/Rv3409c 0.78 0.81 -0.15 -0.6 -0.06 0.09
MB1136c/Rv1106c -5.37 -5.27 -1.34 -2.81 -0.08 -0.47
bovis_lung
bovis_LN
BCG_danish
BCG_pasteur
Mtb_early
Mtb_late
Log2FC
-7.5
-5.0
-2.5
0.0

Lung
Thoracic LN
log10 C
Adj p value <0.05
FALSE
TRUE
phoP
phoR
fadD26
phoP
phoR
fadD26